Highly active catalytic Ru/TiO_2 nanomaterials for continuous production of γ-valerolactone

Weiyi Ouyang,[a] Mario J. Muñoz-Batista,[a] Marcos Fernández-García,[b] and Rafael Luque*[a][c]

Abstract: Green energy production from renewable sources is an attractive but challenging topic to face the likely energy crisis scenario in the future. In the current work, a series of versatile Ru/TiO_2 catalysts were simply synthesized and employed in continuous flow catalytic transfer hydrogenation of industrially derived methyl levulinate biowaste (from Avantium Chemicals B.V.) to γ-valerolactone. Different analytical techniques were applied in the characterization of the as-synthesized catalysts, including XRD, SEM, EDX, TEM and XPS etc. The effects of various reaction conditions (e.g. temperature, concentration and flow rate) were investigated. Results suggested that optimum dispersion and distribution of Ru on the TiO_2 surface could efficiently promote production of γ-valerolactone, with 5% Ru/TiO_2 catalyst providing excelling catalytic performance and stability as compared to commercial Ru catalysts.

Introduction

With the raising of public awareness on environmental protection and climate change, development of green energy, or renewable energy, as alternative to the fossil energy to reduce the carbon emission has drawn intensive attention and become a key issue in the recent decades. In this aspect, massive research efforts have been devoted to the transformation of tremendous biomass into biofuels[1–5] and photocatalytic fuel generations[6–10]. Due to the complexity and recalcitrant of the abundant lignocellulosic biomass, direct transformation of these feedstocks into valuable products (fuels, chemicals and materials) has emerged a bottleneck[11,12], while valorization of carbohydrates derived from lignocellulosic biomass with different strategies has been widely reported[13–22]. Levulinic acid (LA) is one of the most promising primary building block and platform molecules from biomass refinery, which is selected as one of top 12 sugar-derived building blocks[23] and the top 10 chemical opportunities from biorefinery carbohydrates[24] by US Department of Energy (DOE). Therefore, there is great potential to valorize LA and its ester deviriates, alkyl levulinates, into more valuable products, such as γ-valerolatone (GVL).

GVL is considered as one of the most outstanding molecules which can be used as fuel additive, solvent, liquid fuel, and ideal precursor for production of valuable chemicals.[25–29] Notably, hydrogenation of alkyl levulinates to GVL is more preferable because alkyl levulinates have higher production from lignocellulose and are easier for separation when compared with LA.[22,30] Heterogeneous catalysts have been reported to play a key role in the hydrogenation process, most of which are carbon, zeolite and metal oxide supports decorated by transition metals (Au, Co, Cu, Ir, Ni, Pd, Pt, Re, Rh, Ru).[28–39] Especially, Ru catalysts is one of the most widely reported catalyst for hydrogenation of LA and alkyl levulinates because of its outstanding catalytic performance and efficiency because it is one of the most active catalyst for aliphatic carbonyl compounds hydrogenation.[34,40,41] For example, Ru/TiO_2 was reported to be highly efficient in hydrogenation of LA to GVL.[41] However, most of the reported works were performed in batch conditions, and only a few of them were in flow for the hydrogenation of LA instead of alkyl levulinates.[42–47] Considering the advantages of flow reactions (efficient energy utilization, easy scale-up, purification and etc.), it could provide closer view into practical production in industry by mimicking large-scale production on the laboratory scale.[48,49]

The catalytic transformation of alkyl levulinates to GVL via Meerwein–Ponndorf–Verley (MPV) reduction using alcohol as hydrogen donor is highly selective for reducing carbonyl group to alcoholic hydroxyl group.[50–54] Hence, such catalytic transfer hydrogenation (CTH) process offers a simple, efficient and safe option for the valorization of biomass derived molecules using abundant and inexpensive alcohols as hydrogen source and solvent as compared to formic acid and H_2.[51,52,55] For example, 2-propanol was reported to be an active hydrogen donor in the transformation of alkyl levulinates providing good conversion and selectivity.[51,55,56]

In the present work, we reported highly active, selective and stable Ru/TiO_2 catalysts for the continuous flow conversion of biowaste derived methyl levulinate from industrial activities of the company Avantium. TiO_2 was synthesized with reversed micro-emulsion method, while deposition of different Ru content (1, 2, 3, 5 wt.%) was performed using $NaBH_4$ as reducing agent under N_2 bubble production, while the obtained catalysts were denoted as 1% Ru/TiO_2, 2% Ru/TiO_2, 3% Ru/TiO_2 and 5% Ru/TiO_2 accordingly. The catalytic performance of the synthesized materials was tested by catalytic transfer hydrogenation of methyl levulinate (ML) in Phoenix reactor from ThalesNano.

[a] W. Ouyang, Dr. M.J. Munoz-Batista, Prof. R. Luque
Departamento de Química Orgánica
Universidad de Córdoba, Edif. Marie Curie, Ctra Nnal IV-A, Km 396, E14014, Córdoba (Spain)
E-mail: q62alsor@uco.es
[b] Dr. M. Fernández-García
Instituto de Catálisis y Petroleoquímica
CSIC, Marie Curie 2, 28049 Madrid, Spain
Email: mfg@icp.csic.es
[c] Peoples Friendship University of Russia (RUDN University), 6 Miklukho-Maklaya street, Moscow, 117198, Russia

Results and Discussion

Catalysts characterization

XRD patterns of the as-synthesized materials were depicted in

Figure 1, which show that diffraction peaks of all the materials were in good agreement with the identical peaks of pure anatase TiO_2. Pure anatase support, according to previous reports, could favor the selective obtaining of GVL.[56] In detail, the peaks at 2θ

= 25.27 º and 2θ = 48.01º can be ascribed to the {101} and {200} atomic facets respectively.[57,58] The crystal size derived from the {101} peak at 2θ = 25.27 º using Sherrer equation was ca. 16.3 nm for all samples. The crystal cell parameters of the anatase phase TiO_2 derived from the XRD pattern are consistent: a=b=3.78 Å, c=9.49 Å (see details in Table S1). The consistence in the XRD pattern indicates that the deposition of Ru component does not change the crystal structure of TiO_2. This is an expected result due to the relatively mild treatment in comparison with the calcination treatment of the TiO_2 active support. However, no obvious peak for Ru was observed, which can be attributed to the low content and well-dispersion of Ru particles.

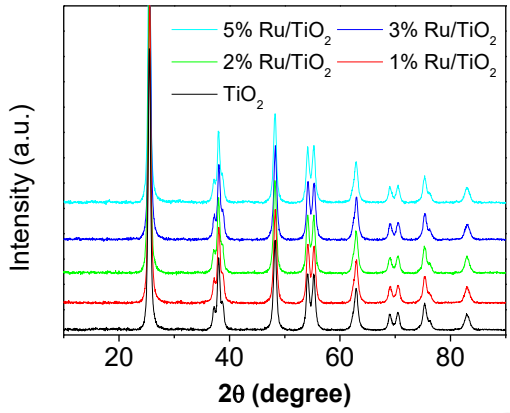

Figure 1 XRD patterns of TiO_2 and Ru/TiO_2 samples

The N_2 absorption-desorption isotherms of the as-synthesized materials were plotted in **Figure 2**, with similar type-IV isotherms featuring a H1 hysteresis loop in the relative pressure range of 0.51-0.89, indicative of typical mesoporous structures[58,59]. The isotherms showed nearly no difference before and after deposition of Ru. BET surface area and average pore size for all materials were found to be in the ca. 40-50 m^2/g and 7.5-7.7 nm range, respectively (see details in Table S1). In conclusion, the high stability of the TiO_2 support detected by XRD, is extensible to all morphological properties of the new materials.

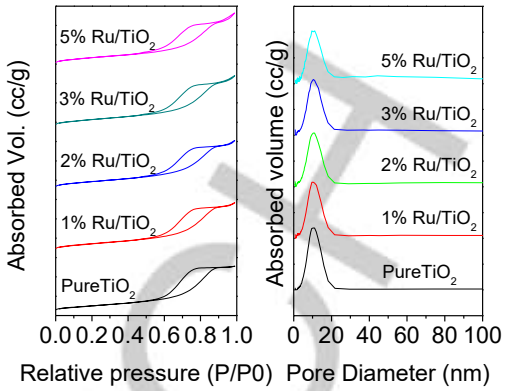

Figure 2 N_2 absorption-desorption isotherms and pore size distribution curves of TiO_2 and Ru/TiO_2 samples

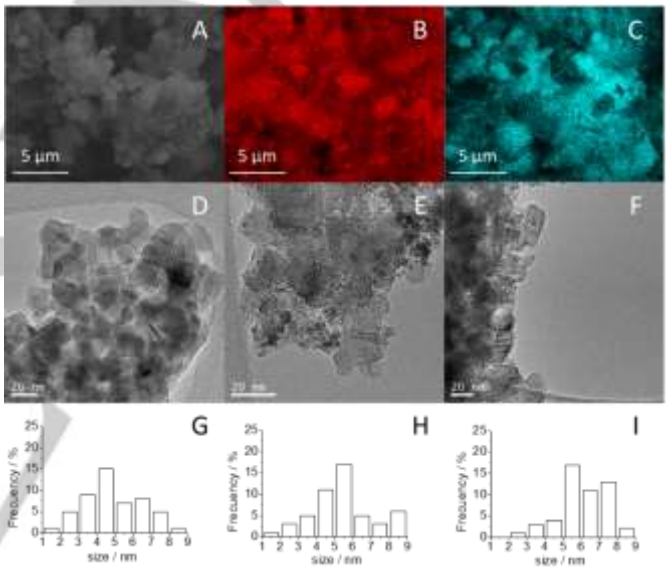

Figure 3 (A) SEM image of 5% Ru/TiO_2; (B) mapping of Ti in (A); (C) mapping of Ru in (A); (D)-(F) TEM images of 2%, 3% and 5% Ru/TiO_2; (G)-(I) Ru particle size distribution

The SEM, TEM image and the element mapping in **¡Error! No se encuentra el origen de la referencia.** show the Ru components were homogeneously and highly dispersed on TiO_2. Additional SEM images and element mapping details can be found in **Figure S1**. The average size of Ru particles was found to be around 5 nm. To investigate the chemical state of synthesized materials, the binding energy in selected region was recorded by XPS. The region of XPS spectra of Ru3d5/2 and Ru3p3/2 overlap with the region of C1s and Ti2p respectively, as shown in

Figure 4 High resolution XPS spectra of (a) C1s/Ru3d region and (c) Ti2p/Ru3p3/2 region of all samples; curve fitting of (b) C1s/Ru3d region and (d) Ti2p/Ru3p3/2 region 5% Ru/TiO_2

. The peak at 280.6 eV in the C1s/Ru3d region (

Figure 4 High resolution XPS spectra of (a) C1s/Ru3d region and (c) Ti2p/Ru3p3/2 region of all samples; curve fitting of (b) C1s/Ru3d region and (d) Ti2p/Ru3p3/2 region 5% Ru/TiO_2

b) can be attributed to Ru (IV), while the fitting peak at ca. 461.3 eV in

Figure 4 High resolution XPS spectra of (a) C1s/Ru3d region and (c) Ti2p/Ru3p3/2 region of all samples; curve fitting of (b) C1s/Ru3d region and (d) Ti2p/Ru3p3/2 region 5% Ru/TiO_2

(d) can be assigned to Ru3p3/2, which is close to the value of Ru(IV), indicating that the RuO_2 is the dominated form in the as-synthesized Ru/TiO_2 samples[60–62]. The splitting value of Ti2p1/2 and Ti2p3/2 is set as 5.7 eV, and the Ti2p3/2 peak locates at 458.1 eV, indicating that Ti was in pure metal oxide form, which is in good agreement with XRD data.

Table 1 Ru contents analysis by EDX and XPS

Catalyst	Ru wt% (from EDX)		Ru/Ti at. % (from XPS)
	fresh	after reaction	
TiO_2	-	-	-
1% Ru/TiO_2	-	-	0.287
2% Ru/TiO_2	-	-	0.409
3% Ru/TiO_2	2.92	2.72	0.432
5% Ru/TiO_2	6.24	5.52	0.697

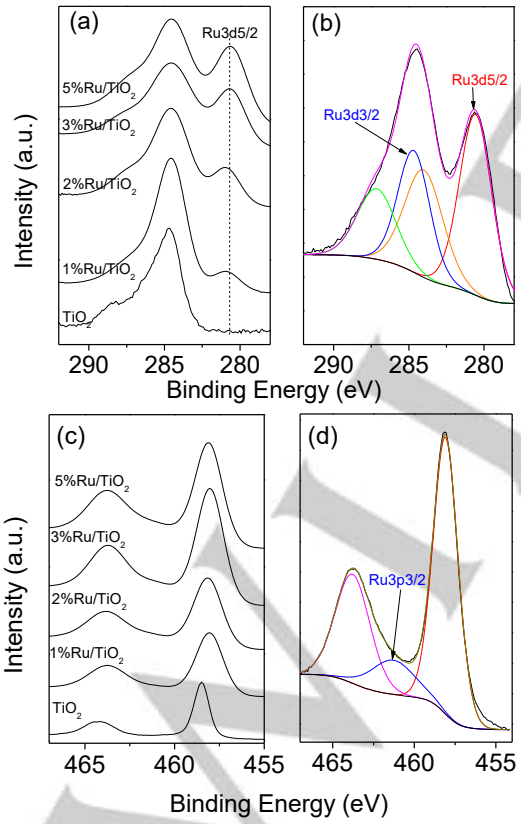

Entry	Catalyst	T (°C)	FR (mL/min)	Conc. (mol	Conv. (%)	Selec. (%)[	Conv. (%)	Selec. (%)[	WHSV[d] (g_{ML}/g	Productivity[e] (mol$_{GVL}$/

Catalytic performance in catalytic transfer hydrogenation of methyl levulinate

2-propanol has been reported as an active hydrogen donor able to provide good conversion and product selectivity as compared with other alcohols including methanol, ethanol, 1-propanol, etc..[55,63] Consequently, 2-propanol was selected as hydrogen donor and solvent for the catalytic transfer hydrogenation of methyl levulinate under continuous flow conditions.

Firstly, the reaction conditions were optimized using 5% Ru/TiO_2 catalyst. By comparing entry 1-5 in **Table 2**, the temperature was observed to be a key factor in the reaction that (the reaction only worked well at 150 °C if the concentration decreased to 0.3 mol/L). As expected, these results indicate that the catalyst possessed a better performance at higher temperatures. Besides, the product selectivity decreased with the increase of inlet flow rate, forming the reaction intermediate - methyl 4-hydroxypentanoate instead of GVL (entry 6-7), which is resulted from the reduced contact time between the reagents and catalysts. The effect of reagent concentration was also investigated, and the results showed that 5% Ru/TiO_2 possess excellent catalytic ability under 200 °C (98% ML conversion, 97% selectivity to GVL). The optimized results included in **Table 2** showed that the highest efficiency in GVL production (ML conv.: 98%, GVL selec.: 97%) was achieved under the following reaction condition: 0.29 g 5% Ru/TiO_2, 0.6 mol/L ML in 2-propanol, 0.3mL/min, 200 °C, 35 bar.

Table 2 Catalytic performance of different catalysts under various reaction conditions [a]

				/L)	[b]	b]	[c]
1	5% Ru/TiO_2	100	0.3	0.3	-	-	/
2	5% Ru/TiO_2	120	0.3	0.3	-	-	/
3	5% Ru/TiO_2	150	0.3	0.3	98	71	/
4	5% Ru/TiO_2	180	0.3	0.3	98	98	/
5	5% Ru/TiO_2	200	0.3	0.3	99	98	/
6	5% Ru/TiO_2	200	0.5	0.3	90	41	/
7	5% Ru/TiO_2	200	0.7	0.3	95	48	/
8	5% Ru/TiO_2	200	1	0.3	-	-	/
9	5% Ru/TiO_2	200	0.3	0.45	98	62	/
10	5% Ru/TiO_2	200	0.3	0.6	96	98	98
11	TiO_2	200	0.3	0.6	-	-	/
12	1% Ru/TiO_2	200	0.3	0.6	28	88	/
13	2% Ru/TiO_2	200	0.3	0.6	85	94	/
14	3% Ru/TiO_2	200	0.3	0.6	95	98	95
15	5% Ru/C	200	0.3	0.6	83	52	25
16	5% Ru/Al_2O_3	200	0.3	0.6	31	97	24

[a] All reactions were performed without catalyst activation. Reaction pressure was set as 35 bar for al reaction conditions. [c] Time-on-stream: 2 h after reaching the reaction conditions. [d] ML weight Productivity was calculated using the hourly molar flow rate of GVL in the effluent divided the mass of F

Subsequently, the reaction was further investigated with both lab-synthesized Ru/TiO_2 catalysts with different Ru loadings and commercial Ru catalysts (5% Ru/C and 5% Ru/Al_2O_3). Results are also summarized in Table 1 (entry 11-16). Notably, TiO_2 itself is not active in the reaction and therefore the reaction performance should be attributed to the incorporated Ru particles. Interestingly, an increase in Ru content on TiO_2 promotes both reaction conversion and selectivity, because of the increase of catalytic sites on the catalyst surface. As compared to lab synthesized catalysts (3% and 5% Ru/TiO_2), a range of commercial catalysts exhibited a significantly reduced activity and selectivity to GVL production (**Table 2Table** , entry 15-16). Most importantly, the catalytic activity of the commercial catalysts also dropped dramatically with time-on-stream (only after 2 h, 3 minutes of residence time of the ML feed in the catalyst), which was found to be related to a larger Ru leaching (See ICP-MS data in **Table 3**) and deactivation under continuous flow conditions. Methyl 4-hydroxypentanoate, reaction intermediate, was observed as major product (selec. >40%, increasing with time on stream) different from GVL when using 5% Ru/C as catalyst. These results pointed out to a reduced hydrogenation ability of Ru/C as compared to the propose Ru/TiO_2 systems to fully hydrogenate ML to GVL. Comparably, the production of isopropyl levulinate (transesterification product) was observed using 5% Ru/Al_2O_3 as catalyst, also increasing with time on stream Hence, the proposed lab-synthesized catalysts outperformed commercial catalysts in the catalytic transfer hydrogenation of methyl levulinate for γ-valerolactone production in terms of activity and stability.

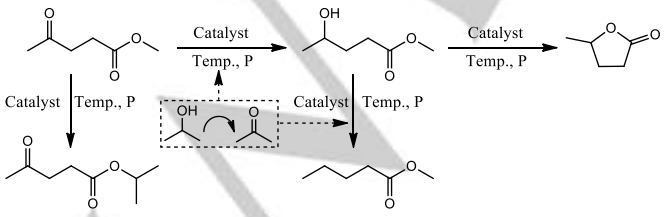

Scheme 1 Possible reaction pathway of catalytic transfer hydrogenation of methyl levulinate using Ru catalysts

According to mass spectra of the obtained samples, we proposed a possible reaction pathway for catalytic transfer hydrogenation of methyl levulinate, which is illustrated in **Scheme 1**. Methyl 4-hydroxypentanoate was firstly formed by partial hydrogenation of the carbonyl group of ML, following by cyclization via transesterification reaction to produce GVL. Meanwhile, transesterification of ML can also proceed, forming isopropyl levulinate, which can be converted to GVL through same reaction pathway as ML.

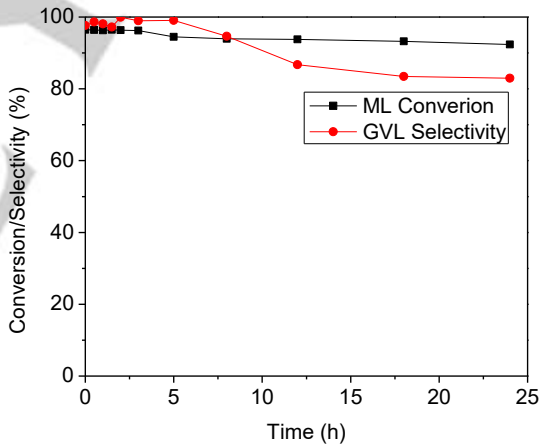

Figure 5 Long term stability test of 5% Ru/TiO_2, 24 h on stream under the optimized condition: 0.29 g 5% Ru/TiO_2, 0.6 mol/L ML in 2-propanol, 0.3mL/min, 200 °C, 35 bar

3% Ru/TiO_2 possessed excellent catalytic performance at the beginning of the reaction, which slightly decreased after 2 hours on stream (ca. 3 min residence time). Long term flow stability study (24 h-36 min residence time-) was subsequently performed for 5% Ru/TiO_2 due to its improved stability and almost negligible Ru leaching. Results from **Figure 5** pointed out a stable conversion of ML (>93%) over 24 hours with only a slight decrease of selectivity from 98% to 83% because of the leaching of catalysts (see **Table 1** and **3**), forming more reaction intermediate, methyl 4-hydroxypentanoate. As shown in **Table 3**,

Ti content was also detected in the outlet stream for the reactions using Ru/TiO_2 catalysts, which could be resulted from the loss of fine catalyt particles smaller than the size of applied membrane filter. The observed GVL productivity is 0.625 $mol_{GVL}/g_{Ru}h$ under the investigated conditions, remarkably superior to that of several systems (not all) previously reported in literature (see **Table 4**). This indicates that 5% Ru/TiO_2 is not only active and selective, but also stable in the transformation of Avantium ML to GVL.

Table 3 Metallic contents in the outlet stream analyzed by ICP-MS [a]

Catalyst	Concentration (μg/L)	
	Ru	Ti
1% Ru/TiO_2 [a]	431.01	330.93
2% Ru/TiO_2 [a]	422.52	256.77
3% Ru/TiO_2 [b]	23.64	435.45
5% Ru/TiO_2 [b]	42.42	300.18
5% Ru/C [a]	1262.52	-
5% Ru/Al_2O_3 [a]	1307.64	-

[a] Samples were taken from the outlet solution collected in 0.5 h after reaching the reaction conditions. [b] Samples were taken from the outlet solution collected in 24 h after reaching the reaction conditions.

Conclusions

Ru/TiO_2 catalysts were successfully synthesized by deposition of RuO_2 nanoparticles onto TiO_2. The presence of RuO_2 nanoparticles on TiO_2 could remarkably promote the catalytic transfer hydrogenation of biomass-derived ML to GVL using 2-propanol as hydrogen donating agent under continuous flow conditions. 5% Ru/TiO_2 showed not only excellent catalytic activity in continuous flow, but also high stability, superior to commercial Ru catalysts in terms of both activity and stability. The above discovery reveals the remarkable potential in the utilization of Ru/TiO_2 catalysts for biomass conversion, especially under flow condition, which may facilitate improved throughput by scaling up. In view of the excelling activity of the proposed systems, the transformation of additional renewable resources into bioenergy can be considered a challenge for further research that will be also reported in due course.

Table 4 Comparison of productivity of GVL from the catalytic conversion of alkyl levulinate

Catalyst	Substanc[a]	H source[b]	Reaction conditions	Conv. (%)	Selec. (%)	Productivity[c] $mol_{GVL}/g_{metal}h$	Ref.
			Flow reaction				
5% Ru/TiO_2	ML	2-PrOH	0.6 M ML in 2-PrOH, 200 °C, 35 bar, 0.3 mL/min, WHSV=2.34 h^{-1}	93.15	90.14	0.625[d]	This work
5% Ru/C	BL	1-BuOH	1 M BL& 6 M H_2O in 1-butanol, 150 °C, 35 bar, WHSV=0.9 h^{-1}	91	89	0.085	[64]
20-Cu/Al_2O_3	ML	H_2	Pure ML feed rate of 1.65 g/h, H_2 flow of 30 mL/min.	93.7	91.5	0.109	[65]
ZrO_2	BL	2-PrOH	5 wt % BL in 2-PrOH, 180 °C, 300 psig He, WHSV = 0.18 h^{-1}	93.2	86.4	0.0065[e]	[66]
			Batch reaction				
$Zr(OH)_4$	EL	EtOH	1g catalysts, 2 g EL, 38 g ethanol, 240 °C, purged with N_2 at atmospheric conditions	89.1	84.5	0.01 [e]	[51]
RANEY® Ni	EL	2-PrOH	0.03 g catalysts, 1 mmol EL, 2-PrOH, room temperature, Ar, 9 h	-	-	0.074	[55]
5% Ru/C	ML	H_2	0.025 g catalysts, 17.2 mmol ML, 10 g MeOH, 120 °C, 30 bar H_2, 5 h	100	82	2.257	[67]
5% Ru/C	ML	H_2	0.025 g catalysts, 0.43 M ML in MeOH, 130 °C, 12 bar H_2, 2.66 h	97.8	89.4	1.12	[68]
Ni1Zr1O	ML	H_2	0.05 g catalysts, 0.15 g ML, 5.0 g H_2O, 3 bar H_2, 3 h.	>99	98.2	0.0075[e]	[69]
red-oxd-Ni/CNHs	ML	2-PrOH	0.1 g catalysts, 24 mL of 0.2 M ML in 2-PrOH, 200 °C, 3 h	96.2	93	0.0397	[70]
CuCr	ML	H_2	0.2 g catalysts, 20 g ML, 250 °C 40 bar H_2, 4 h	95	97.6	0.178[e]	[71]
Ni-$Fe_{0.5}$/AC	EL	H_2	0.04 g catalysts, 0.1 g EL, 10 mL H_2O, 100 °C, 6 h, 40 bar	99.3	99	0.0406	[72]
ZrFeO(1:1)-300	EL	2-PrOH	0.2 g catalysts, 0.65 g EL, 11.8 g 2-PrOH, 230 °C, 52 bar, 0.5 h	94.2	92	0.039[e]	[73]
10Cu-5Ni/Al_2O_3	ML	2-BuOH	0.1 catalysts, 1 mmol ML, 3 mL 2-BuOH, 150 °C, 12 h, purged with N_2 at atmospheric conditions	100	97	0.0539	[74]
Zr-HA	EL	2-PrOH	0.2 g catalysts, 1 mmol EL, 5 mL 2-PrOH, 150 °C, 3 h	86.4	87.7	0.000758[e]	[75]
1% Pt/ZSM-35	EL	H_2	0.1 g catalysts,1.0 mmol EL, 12 mL ethanol, 60 bar H_2, 200 °C, 6 h	100	99	0.165	[76]
Co	EL	H_2	0.1 g catalysts, 1 g EL,130 °C, 33 bar H_2, 3 h	99	95	0.024	[30]
CuO	ML	MeOH	0.3 g catalysts, 8 mmol ML, 19.5 g MeOH, 1 h	97.6	87.6	0.0228	[77]
4% $Ru(OH)_x/TiO_2$(A)	ML	2-PrOH	0.1 g catalysts, 1 mmol ML, 5 mL 2-PrOH, 90 °C, 24 h, Ar	100	99	0.236	[56]
ZrO_2(10)/SBA-15	ML	2-PrOH	Catalyst (40 mg as ZrO_2), 2 mmol ML, 10 mL 2-PrOH, 150◦C, Ar (10 bar), 3 h	>99.5	91	15.2[f]	[63]
Zr-HBA	EL	2-PrOH	0.2 g catalysts, 1 mmol EL, 100 mmol 2-PrOH, 150 °C, 4 h	100	94.4	0.0012	[27]

[a] ML: methyl levulinate; EL: ethyl levulinate; BL: butyl levulinate. [b] MeOH: methanol; EtOH: ethanol; 2-PrOH: 2-propanol; 1-BuOH: 1-butanol; 2-BuOH: 2-butanol. [c] Calculated from literature data, using the mass of metal of a given catalyst. [d] Calculated from the average conversion and selectivity values. [e] Calculated from literature data, using the mass of catalyst. [f] Calculated based on the mass of ZrO_2.

Experimental Section

Synthesis of TiO_2

TiO_2 was synthesized with reversed micro-emulsion method.[78] In detail, 177.4 mL triton (surfactant) and 185.4 mL of hexanol (co-surfactant) were

added into 854 mL n-heptane and stirred at 400 rpm for 30 minutes. Subsequently, 100 mL MiliQ water was added to the above solution, then the resulted mixture was stirred for 1 hour. Meanwhile, 14.7 mL titanium isopropoxide (TTIP) was dissolved into 24.4 mL 2-propanol, which was then added into the previous mixture drop by drop. The obtained mixture was kept stirring at 400 rpm for overnight, following by centrifugation at 10000 rpm, 4 ºC for 15 minutes for removal of dispersion phase. Afterwards, the obtained solids were washed with methanol under stirring at 400 rpm for 15 minutes and recovered by centrifugation under same condition. Finally, the white solids were dried at 80 ºC for overnight, and then calcined at 600 ºC for 30 minutes with ramping rate of 1 ºC/min.

Deposition of Ru onto TiO_2

0.5 g TiO_2 was added to 100 mL MilliQ water and then the mixture was sonicated for 30 minutes. Subsequently, different amount of $RuCl_3 \cdot xH_2O$ was added to the mixture with another 5 minutes' sonication. Then, different amount of 0.1 mol/L $NaBH_4$ solution (molar ratio, Ru^{3+}:BH^{-1} = 1:5) was added to the mixture as reducing agent with stirring for 1 hour. The whole synthesis was protected under N_2 bubbling. After the synthesis, the solids were separated by centrifugation (13000 rpm, 10 min, 4 ºC) and washed with DI water. The obtained solids were dried at 80 ºC for overnight.

Catalysts characterization

XRD patterns were recorded with a Seifert D-500 diffractometer using Ni-filtered Cu Kα radiation with a 0.02° step and fitted using the Von Dreele approach to the Le Bail method. BET surface area and porosity analysis were performed in Micromeritics ASAP 2010 by nitrogen physisorption. Scanning electron microscopy images were recorded with a JEOL JSM-7800 scanning microscope equipped with EDX at 20 kV in SCAI of Universidad de Cordoba. An Au/Pd coating was employed to analyze samples on a high-resolution sputtering SC7640 instrument (up to 7 nm thickness) at a sputtering rate of 1.5 kV per minute. TEM analysis of the materials was carried out with a JEOL 2100F TEM/STEM microscope. X-ray photoelectron spectroscopy (XPS) measurements were performed in a VG Scientific photoelectron spectrometer ESCALAB-210 equipped with Mg Kα radiation (1486.6 eV) from an X-ray source, operated at 15 kV and 20 mA. Survey spectra in the energy range from 0 to 1350 eV were recorded using 0.4 eV steps for all the samples. High resolution spectra were recorded with 0.1 eV steps, 100 ms dwell time and 25 eV pass energy. Catalyst leaching was analyzed by ICP-MS in SCAI of Universidad de Cordoba. 1 mL of the selected samples were transferred to 25 mL falcon tube and dried in oven to evaporate the organic compounds. Then, 1 mL of HCl (≥37%), HF (47-51%) and HNO_3 (≥69%) was added to digest the solids, and subsequently diluted into 15 mL aqueous solution for analysis. Samples were then immediately analyzed in an ICP/MS Perkin Elmer ELAN-DRC-e model equipped with an automatic diluting injecting system and ionization under Ar plasma followed by quadrupole ion detection with a DRC cell to remove potential interferences.

Hydrogenation of methyl levulinate in continuous flow

Catalytic transfer hydrogenation of methyl levulinate was performed in the liquid phase continuous flow reactor, Phoenix from ThalesNano Inc. using ca. 300 mg catalysts. Feedstock solutions were prepared by diluting methyl levulinate (>99%, kindly donated by Avantium as side product of their YXY process, https://www.avantium.com/yxy/yxy-technology/) in 2-propanol at the desired concentration. Reaction optimization was performed in various conditions: concentration (0.3M, 0.45 M, 0.6M), temperature (100, 120, 150, 180, 200 ºC), flow rate (0.3, 0.5, 0.7, 1 mL/min). The optimized conditions were 0.6M methyl levulinate, 200 ºC, 35 bar and 0.3 mL/min, which the WHSV was around 4.69 h^{-1}. Catalysts with different Ru loadings were employed under optimized conditions. Long term stability runs for the optimum catalyst and conditions were performed by streaming for 24 hours. The obtained samples were analyzed by GC Agilent 5890 Series II equipped with FID detector using SUPELCO EQUITY TM-1 fused silica capillary column (60 m × 0.25 mm × 0.25 μm). Both the injector temperature and detector temperature were 250 ºC. Initial oven temperature was 60 ºC (held for 1 min), and then increased to 230 ºC with ramping rate of 10 ºC/min and held for 5 min. Decane was used as internal standard in GC analysis. GC-MS equipped with HP-5 column from SCAI of Universidad de Cordoba was used for the analysis of the products. Temperature of injector and detector was set as 250 ºC. Initial oven temperature was 60 ºC (held for 1 min), then increased to 230 ºC with ramping rate of 10 ºC/min and held for 5 min, and finally increased to 280 ºC with ramping rate of 30 ºC/min and held for 2 min. Conversion, selectivity and productivity were calculated as below:

$$Conversion = \frac{(C_{ML,initial} - C_{ML,final})}{C_{ML,initial}} \times 100\%$$

$$Selectivity = \frac{C_{GVL}}{C_{ML,initial} - C_{ML,final}} \times 100\%$$

$$Productivity = \frac{hourly\ molar\ flow\ rate\ of\ GVL}{m_{Ru}}$$

Acknowledgements

Rafael Luque gratefully acknowledges Consejería de Ciencia e Innovación, Junta de Andalucía for funding project P10-FQM-6711. Funding from Marie Curie Actions under Innovative Training Networks Project Photo4Future (H2020-MSCA-ITN-2014-641861), especially for funding Weiyi Ouyang Ph.D. studies is gratefully acknowledged. The ICP group thanks MINECO (Spain) financial support through the ENE2016-77798-C4-1-R project. Mario J. Munoz-Batista gratefully acknowledges MINECO for a JdC contract (Ref. FJCI-2016-29014). Special thanks to ThalesNano Inc. for providing the commercial catalysts and to Avantium Chemicals BV for the generous supply of methyl levulinate.

Keywords: ruthenium • titanium • heterogeneous catalysis • hydrogenation • methyl levulinate• γ-valerolactone • flow chemistry

[1] M. He, Y. Sun, B. Han, *Angew. Chemie - Int. Ed.* **2013**, *52*, 9620–9633.

[2] R. Rinaldi, R. Jastrzebski, M. T. Clough, J. Ralph, M. Kennema, P. C. A. Bruijnincx, B. M. Weckhuysen, *Angew. Chemie Int. Ed.* **2016**, *55*, 8164–8215.

[3] A. Corma, S. Iborra, A. Velty, *Chem. Rev.* **2007**, *107*, 2411–2502.

[4] G. W. Huber, S. Iborra, A. Corma, *Chem. Rev.* **2006**, *106*, 4044–

4098.

[5] R. D. Perlack, L. L. Wright, A. F. Turhollow, R. L. Graham, B. J. Stokes, D. C. Erbach, *Agriculture* **2005**, *DOE/GO-102*, 78.

[6] Y. Ma, X. Wang, Y. Jia, X. Chen, H. Han, C. Li, *Chem. Rev.* **2014**, *114*, 9987–10043.

[7] A. Le Goff, V. Artero, B. Jousselme, P. D. Tran, N. Guillet, R. Metaye, A. Fihri, S. Palacin, M. Fontecave, *Science (80-.).* **2009**, *326*, 1384–1387.

[8] J. Zhang, J. Yu, Y. Zhang, Q. Li, J. R. Gong, *Nano Lett.* **2011**, *11*, 4774–4779.

[9] X. Zong, H. Yan, G. Wu, G. Ma, F. Wen, L. Wang, C. Li, *J. Am. Chem. Soc.* **2008**, *130*, 7176–7177.

[10] Q. Xiang, J. Yu, M. Jaroniec, *J. Am. Chem. Soc.* **2012**, *134*, 6575–6578.

[11] X. Zhao, L. Zhang, D. Liu, *Biofuels, Bioprod. Biorefining* **2012**, *6*, 465–482.

[12] S. Saravanamurugan, A. Riisager, *ChemCatChem* **2013**, *5*, 1754–1757.

[13] C. O. Tuck, E. Perez, I. T. Horvath, R. a. Sheldon, M. Poliakoff, *Science (80-.).* **2012**, *337*, 695–699.

[14] J. N. Chheda, G. W. Huber, J. A. Dumesic, *Angew. Chemie Int. Ed.* **2007**, *46*, 7164–7183.

[15] J. C. Serrano-Ruiz, R. Luque, A. Sepúlveda-Escribano, *Chem. Soc. Rev.* **2011**, *40*, 5266–5281.

[16] R. Luque, J. C. Lovett, B. Datta, J. Clancy, J. M. Campelo, A. a. Romero, *Energy Environ. Sci.* **2010**, *3*, 1706–1721.

[17] V. Budarin, R. Luque, D. J. Macquarrie, J. H. Clark, *Chem. - A Eur. J.* **2007**, *13*, 6914–6919.

[18] C. Len, R. Luque, *Sustain. Chem. Process.* **2014**, *2*, 1.

[19] H. Li, Z. Fang, J. Luo, S. Yang, *Appl. Catal. B Environ.* **2017**, *200*, 182–191.

[20] C.-H. Kuo, A. S. Poyraz, L. Jin, Y. Meng, L. Pahalagedara, S.-Y. Chen, D. A. Kriz, C. Guild, A. Gudz, S. L. Suib, *Green Chem.* **2014**, *16*, 785–791.

[21] X. Hu, C.-Z. Li, *Green Chem.* **2011**, *13*, 1676–1679.

[22] F. Yu, R. Zhong, H. Chong, M. Smet, W. Dehaen, B. F. Sels, *Green Chem.* **2017**, *19*, 153–163.

[23] T. Werpy, G. Petersen, *Top Value Added Chemicals from Biomass: Volume I -- Results of Screening for Potential Candidates from Sugars and Synthesis Gas*, Golden, CO, **2004**.

[24] J. J. Bozell, G. R. Petersen, *Green Chem.* **2010**, *12*, 539–554.

[25] D. M. Alonso, S. G. Wettstein, J. A. Dumesic, *Green Chem.* **2013**, *15*, 584–595.

[26] J. Q. Bond, D. M. Alonso, D. Wang, R. M. West, J. a Dumesic, *Science (80-.).* **2010**, *327*, 1110–1114.

[27] J. Song, L. Wu, B. Zhou, H. Zhou, H. Fan, Y. Yang, Q. Meng, B. Han, *Green Chem.* **2015**, *17*, 1626–1632.

[28] W. R. H. Wright, R. Palkovits, *ChemSusChem* **2012**, *5*, 1657–1667.

[29] K. Yan, Y. Yang, J. Chai, Y. Lu, *Appl. Catal. B, Environ.* **2015**, *179*, 292–304.

[30] H. Zhou, J. Song, H. Fan, B. Zhang, Y. Yang, J. Hu, Q. Zhu, B. Han, *Green Chem.* **2014**, *16*, 3870–3875.

[31] K. Yan, A. Chen, *Energy* **2013**, *58*, 357–363.

[32] M. Sudhakar, V. V. Kumar, G. Naresh, M. L. Kantam, S. K. Bhargava, A. Venugopal, *Appl. Catal. B Environ.* **2016**, *180*, 113–120.

[33] E. V. Starodubtseva, O. V. Turova, M. G. Vinogradov, L. S. Gorshkova, V. A. Ferapontov, *Russ. Chem. Bull.* **2007**, *56*, 552–554.

[34] C. Ortiz-Cervantes, J. J. García, *Inorganica Chim. Acta* **2013**, *397*, 124–128.

[35] H. Zhou, J. Song, X. Kang, J. Hu, Y. Yang, H. Fan, Q. Meng, B. Han, *RSC Adv.* **2015**, *5*, 15267–15273.

[36] P. P. Upare, J.-M. Lee, D. W. Hwang, S. B. Halligudi, Y. K. Hwang, J.-S. Chang, *J. Ind. Eng. Chem.* **2011**, *17*, 287–292.

[37] J. M. Bermudez, J. A. Menéndez, A. A. Romero, E. Serrano, J. Garcia-Martinez, R. Luque, *Green Chem.* **2013**, *15*, 2786–2792.

[38] A. M. Hengne, C. V. Rode, *Green Chem.* **2012**, *14*, 1064–1072.

[39] R. Yoshida, D. Sun, Y. Yamada, S. Sato, G. J. Hutchings, *Catal. Commun.* **2017**, *97*, 79–82.

[40] P. Kluson, L. Cerveny, *Appl. Catal. A-General* **1995**, *128*, 13–31.

[41] A. Primo, P. Concepcion, A. Corma, *Chem. Commun.* **2011**, *47*, 3613–3615.

[42] O. A. Abdelrahman, A. Heyden, J. Q. Bond, *ACS Catal.* **2014**, *4*, 1171–1181.

[43] J. Wang, S. Jaenicke, G.-K. Chuah, *RSC Adv.* **2014**, *4*, 13481–13489.

[44] C. Moreno-Marrodan, P. Barbaro, *Green Chem.* **2014**, *16*, 3434–3438.

[45] P. Azadi, R. Carrasquillo-Flores, Y. J. Pagán-Torres, E. I. Gürbüz, R. Farnood, J. A. Dumesic, *Green Chem.* **2012**, *14*, 1573–1576.

[46] J. M. Tukacs, R. V. Jones, F. Darvas, G. Dibó, G. Lezsák, L. T. Mika, *RSC Adv.* **2013**, *3*, 16283–16287.

[47] A. S. Piskun, J. E. de Haan, E. Wilbers, H. H. van de Bovenkamp, Z. Tang, H. J. Heeres, *ACS Sustain. Chem. Eng.* **2016**, *4*, 2939–2950.

[48] J. Wegner, S. Ceylan, A. Kirschning, *Adv. Synth. Catal.* **2012**, *354*, 17–57.

[49] L. Vaccaro, D. Lanari, A. Marrocchi, G. Strappaveccia, *Green Chem.* **2014**, *16*, 3680–3704.

[50] V. Polshettiwar, R. S. Varma, *Green Chem.* **2009**, *11*, 1313–1316.

[51] X. Tang, H. Chen, L. Hu, W. Hao, Y. Sun, X. Zeng, L. Lin, S. Liu, *Appl. Catal. B Environ.* **2014**, *147*, 827–834.

[52] J. He, H. Li, Y. Lu, Y. Liu, Z. Wu, D. Hu, S. Yang, *Appl. Catal. A Gen.* **2016**, *510*, 11–19.

[53] H. Y. Luo, D. F. Consoli, W. R. Gunther, Y. Román-Leshkov, *J. Catal.* **2014**, *320*, 198–207.

[54] A. Osatiashtiani, A. F. Lee, K. Wilson, *J. Chem. Technol. Biotechnol.* **2017**, *92*, 1125–1135.

[55] Z. Yang, Y.-B. Huang, Q.-X. Guo, Y. Fu, *Chem. Commun.* **2013**, *49*, 5328–5330.

[56] Y. Kuwahara, W. Kaburagi, T. Fujitani, *RSC Adv.* **2014**, *4*, 45848–45855.

[57] H. G. Yang, C. H. Sun, S. Z. Qiao, J. Zou, G. Liu, S. C. Smith, H. M. Cheng, G. Q. Lu, *Nature* **2008**, *453*, 638–641.

[58] Y. Cao, Q. Li, C. Li, J. Li, J. Yang, *Appl. Catal. B Environ.* **2016**, *198*, 378–388.

[59] J. Wang, Z. Bian, J. Zhu, H. Li, *J. Mater. Chem. A* **2013**, *1*, 1296–1302.

[60] E. A. Paoli, F. Masini, R. Frydendal, D. Deiana, C. Schlaup, M.

Malizia, T. W. Hansen, S. Horch, I. E. L. Stephens, I. Chorkendorff, *Chem. Sci.* **2015**, *6*, 190–196.

[61] C. Bock, C. Paquet, M. Couillard, G. A. Botton, B. R. MacDougall, *J. Am. Chem. Soc.* **2004**, *126*, 8028–8037.

[62] J. W. Guo, T. S. Zhao, J. Prabhuram, R. Chen, C. W. Wong, *Electrochim. Acta* **2005**, *51*, 754–763.

[63] Y. Kuwahara, W. Kaburagi, Y. Osada, T. Fujitani, H. Yamashita, *Catal. Today* **2017**, *281*, 418–428.

[64] E. I. Gurbuz, D. M. Alonso, J. Q. Bond, J. A. Dumesic, *ChemSusChem* **2011**, *4*, 357–361.

[65] D. Sun, A. Ohkubo, K. Asami, T. Katori, Y. Yamada, S. Sato, *Mol. Catal.* **2017**, *437*, 105–113.

[66] M. Chia, J. A. Dumesic, *Chem. Commun.* **2011**, *47*, 12233–12235.

[67] L. Negahdar, M. G. Al-Shaal, F. J. Holzhäuser, R. Palkovits, *Chem. Eng. Sci.* **2017**, *158*, 545–551.

[68] M. G. Al-Shaal, W. R. H. Wright, R. Palkovits, *Green Chem.* **2012**, *14*, 1260–1263.

[69] M. Sun, J. Xia, H. Wang, X. Liu, Q. Xia, Y. Wang, *Appl. Catal. B Environ.* **2018**, *227*, 488–498.

[70] C. Termvidchakorn, K. Faungnawakij, S. Kuboon, T. Butburee, N. Sano, T. Charinpanitkul, *Appl. Surf. Sci.* **2018**, DOI 10.1016/j.apsusc.2018.04.054.

[71] Z. Li, M. Zuo, Y. Jiang, X. Tang, X. Zeng, Y. Sun, T. Lei, L. Lin, *Fuel* **2016**, *175*, 232–239.

[72] C. Li, G. Xu, Y. Zhai, X. Liu, Y. Ma, Y. Zhang, *Fuel* **2017**, *203*, 23–31.

[73] H. Li, Z. Fang, S. Yang, *ACS Sustain. Chem. Eng.* **2016**, *4*, 236–246.

[74] B. Cai, X.-C. Zhou, Y.-C. Miao, J.-Y. Luo, H. Pan, Y.-B. Huang, *ACS Sustain. Chem. Eng.* **2017**, *5*, 1322–1331.

[75] Z. Xiao, H. Zhou, J. Hao, H. Hong, Y. Song, R. He, K. Zhi, Q. Liu, *Fuel* **2017**, *193*, 322–330.

[76] C.-B. Chen, M.-Y. Chen, B. Zada, Y.-J. Ma, L. Yan, Q. Xu, W.-Z. Li, Q.-X. Guo, Y. Fu, *RSC Adv.* **2016**, *6*, 112477–112485.

[77] X. Tang, Z. Li, X. Zeng, Y. Jiang, S. Liu, T. Lei, Y. Sun, L. Lin, *ChemSusChem* **2015**, *8*, 1601–1607.

[78] M. J. Muñoz-Batista, A. Kubacka, M. Fernández-García, *ACS Catal.* **2014**, *4*, 4277–4288.

Entry for the Table of Contents

Layout 1:

FULL PAPER

Efficient green energy production from biomass derived building block: Ru/TiO_2 catalysts were successfully synthesized and employed in the transformation of biomass derived methyl levulinate into to γ-valerolactone. Superior catalytic performance as compared to the commercial catalysts was observed, revealing a great potential for green energy production from renewable resources.

Weiyi Ouyang,[a] Mario J. Muñoz-Batista,[a] Marcos Fernandez-Garcia,[b] and Rafael Luque[a][c]*

Page No. – Page No.

Highly active catalytic Ru/TiO_2 nanomaterials for continuous production of γ-valerolactone